SUPPLEMENTARY DATA

Multispline catheter mapping of the coronary ostia to guide ablation at the aortic root

Cartografía de los *ostium* de arterias coronarias con catéter multipolar para guiar la ablación en la raíz aórtica

1. Supplementary methods: Classification model

A classification model was developed to predict the proximity between ablation lesions and CT-identified coronary ostia (LCA or RCA) using ECG-derived features, aiming to address the anticipated difficulty in engaging the RCA ostium electroanatomically. Proximity was defined a priori as "near" if the CT distance was < 10 mm and "far" otherwise, in line with guideline safety thresholds. Thirteen direct ECG metrics and three literature-based composite indices were evaluated as candidate predictors.

A Gradient Boosting Machine was trained with repeated stratified cross-validation (5 folds, 10 repetitions). For each repetition, out-of-fold (OOF) predictions were obtained for each patient (predictions from models that did not see that case) and then averaged across repetitions to yield 1 seed-independent probability of "near" per patient.

To prioritize safety, the classifier operated at a sensitivity-oriented decision threshold: p_cut was defined as the 5th percentile of the OOF probabilities among clinically "near" cases (<10 mm). Thus, ≈95% of truly "near" cases were expected to have p≥p_cut in this cohort, reducing false negatives at the expense of more false positives. Cases were finally labelled "near" if p≥p_cut and "far" otherwise.

The primary metric was the F1-score; secondary metrics included precision, recall, accuracy, and precision–recall AUC (PR-AUC) (preferred over ROC-AUC given class imbalance). Uncertainty for PR-AUC was quantified with non-parametric bootstrap 95%

confidence intervals computed on the per-patient OOF predictions (stratified resampling, 2,000 replicates).

Feature importance was summarized using GBM relative influence (caret varImp).

Analyses were performed in R 4.3.1 using caret (data partitioning, preprocessing, training/validation), gbm (gradient boosting), ggplot2 (plots), and readxl/dplyr (data handling). GBM hyperparameters were: n.trees = 200, interaction.depth = 2, shrinkage = 0.05, n.minobsinnode = 2, bag.fraction = 1. Centering and scaling were applied within each resample.

2. Supplementary results: Classification model

Figures S6–S7 display, for each patient, the averaged out-of-fold (OOF) probability of being *near*, plotted against the true class for LCA and RCA. Points are color-coded as: green (correct), red (false negative), and orange (false positive). A dashed horizontal line marks the sensitivity-oriented threshold (p_cut). Performance summaries (F1, precision, recall, accuracy, and PR-AUC) are computed from these averaged OOF probabilities at this operating point; 95% bootstrap CIs are shown in **Table S3**.

3. Supplementary tables

Table S1. ECG derived measurement and indices

Variable	Description	Variable	Description
X1	PVC transition score	X9	S-wave amplitude in V2 during PVC
X2	NSR transition score	X10	QRS amplitude in V2 during PVC
X3	Transition index	X11	R-wave amplitude in V2 during NSR
X4	Maximal R-wave width during PVC in V_1 or V_2	X12	QRS amplitude in V2 during NSR
X5	PVC QRS width	X13	R-wave amplitude in V3 during PVC
X6	R-wave amplitude in V_1 during PVC	XI1	V2/V3 amplitude index
X7	R-wave amplitude in V_2 during PVC	XI2	Betensky index: (R / [R + S]) in PVC vs. NSR
X8	S-wave amplitude in V_1 during PVC	XI3	R-wave duration index (R/S ratio)

Table S2. Baseline characteristics of the study population stratified by site of origin of PVCs

Location	Nonsummit origin			Summit	Full cohort	P*
	LCC-RCC commissure N=24	LCC - AMC N=13	RCC N=7	N=7	N=51	
Age, y	60 [55-68]	68 [58-71]	64 [51-72]	64 [55-80]	62 [56-70]	.784
LVEF, %	55 [47-60]	54 [45-58]	60 [58-60]	50 [45-55]	55 [45-60]	.194
LVEDV, mL	169 [147-198]	176 [160-205]	153 [147-160]	164 [135-164]	165 [147-198]	.494
Idiopathic	17 [71]	8 [62]	6 [86]	3 [43]	34 [67]	.203
Female	10 [42]	5 [38]	4 [57]	2 [29]	21 [41]	.685
Distance LCA, mm	14.1 [10.5-17.2]	10.2 [7.1-13.7]	24.2 [17.5-38.5]	16.0 [13.3-22.8]	14.5 [10.2-22.8]	.353
Distance RCA, mm	19.6 [15.0-25.0]	23.7 [21.8-28.0]	9.3 [5.1-23.4]	24.7 [23.8-32.0]	22.1 [16.0-26.0]	.020

AMC, aortomitral continuity; LCA, left coronary artery; LCC, left coronary cusp; LVEDV, left ventricular end-diastolic volume; LVEF, left ventricular ejection fraction; PVCs, premature ventricular contractions; RCA, right coronary artery; RCC, right coronary cusp.

The data are expressed as No. (%) or median [25th-75th percentile range].

*Comparisons were made between patients with and without PVC origin in the left ventricular summit.

Table S3. Performance at the sensitivity-oriented threshold (p_cut)

Artery	Near/total	Precision	Recall	F1	Accuracy	PR-AUC (95% CI)	TP/FP/TN/FN
LCA	9/39	0.237	1.000	0.383	0.256	0.406 (0.154-0.682)	9 / 29 / 1 / 0
RCA	4 / 35	0.571	1.000	0.727	0.914	0.369 (0.232–1.000)	4 / 3 / 28 / 0

CI, confidence interval; FN, false negative; FP, false positive; LCA, left coronary artery; Near, < 10 mm from the coronary ostium; OOF, out-of-fold; PR-AUC, precision-recall area under the curve; RCA, right coronary artery; TN, true negative; TP, true positive.

4. Supplementary figures

Figure S1: Integration of cardiac CT images into the electroanatomic mapping system (CARTO3). Image fusion is performed in two steps: (1) landmark registration using three anatomically defined intracardiac locations to approximate the spatial orientation of the CT dataset, followed by (2) surface registration, which applies an algorithm that minimizes the mean distance between the CT-derived anatomical shell and the catheter-acquired electroanatomic map, enabling more accurate geometric alignment. Fusion of the aorta, right ventricle, and left ventricle is shown.

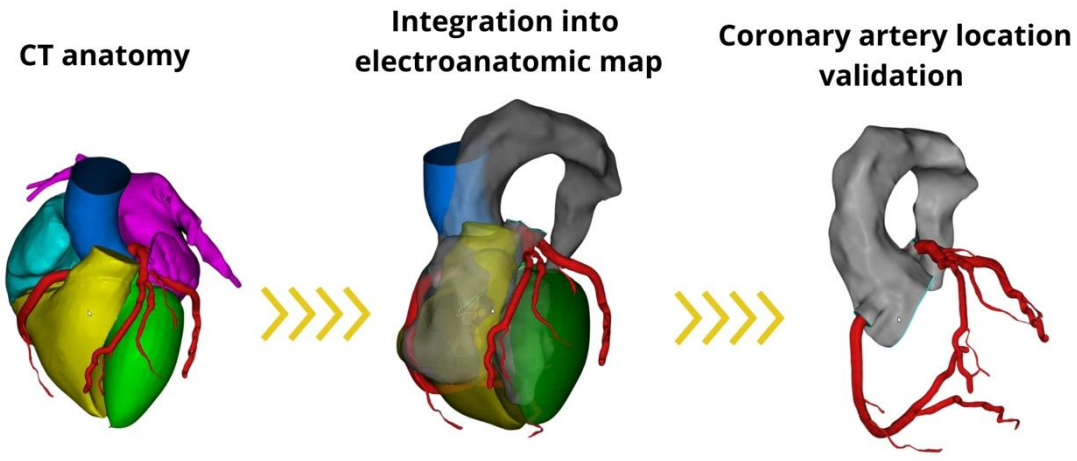

Figure S2. Flow diagram of patient inclusion.

CT, computed tomography; GB, Gradient Boosting; LBBB, left bundle branch block; PAD, peripheral arterial disease; PVC, premature ventricular contraction; RCA, right coronary artery.

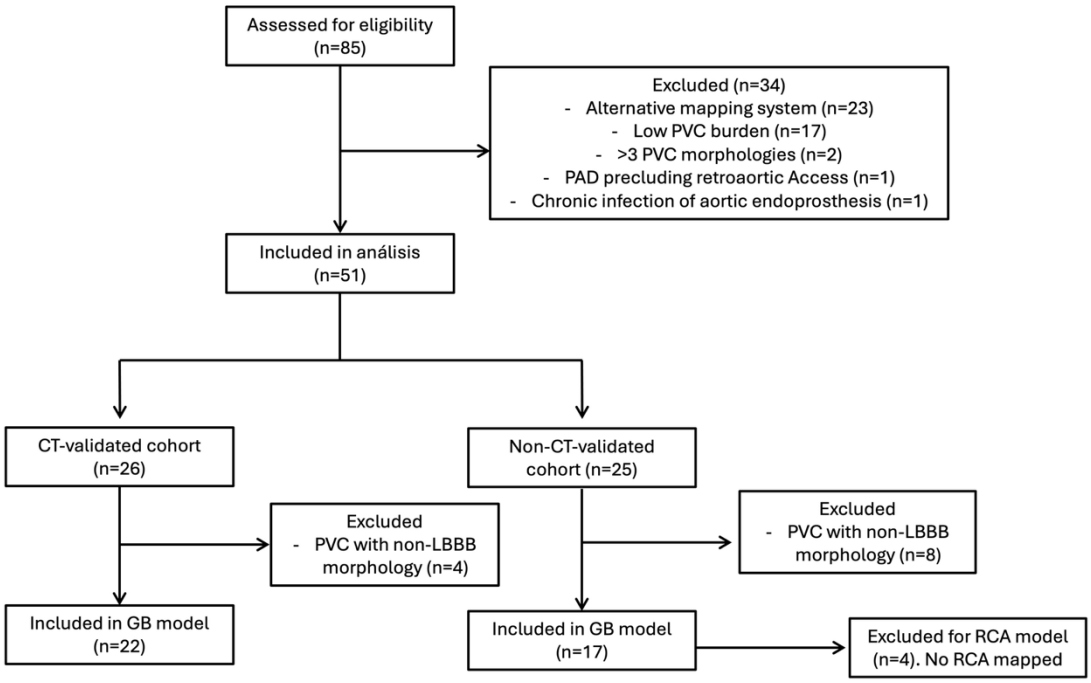

CT, computed tomography; GB, Gradient Boosting; LBBB, left bundle branch block; PAD, peripheral arterial disease; PVC, premature ventricular contraction; RCA, right coronary artery.

Figure S3. Relative importance of variables included in the predictive model for the proximity between ablation lesions and the left coronary artery (LCA) ostium, based on segmentation obtained by computed tomography. Variable codes are defined in Table S1.

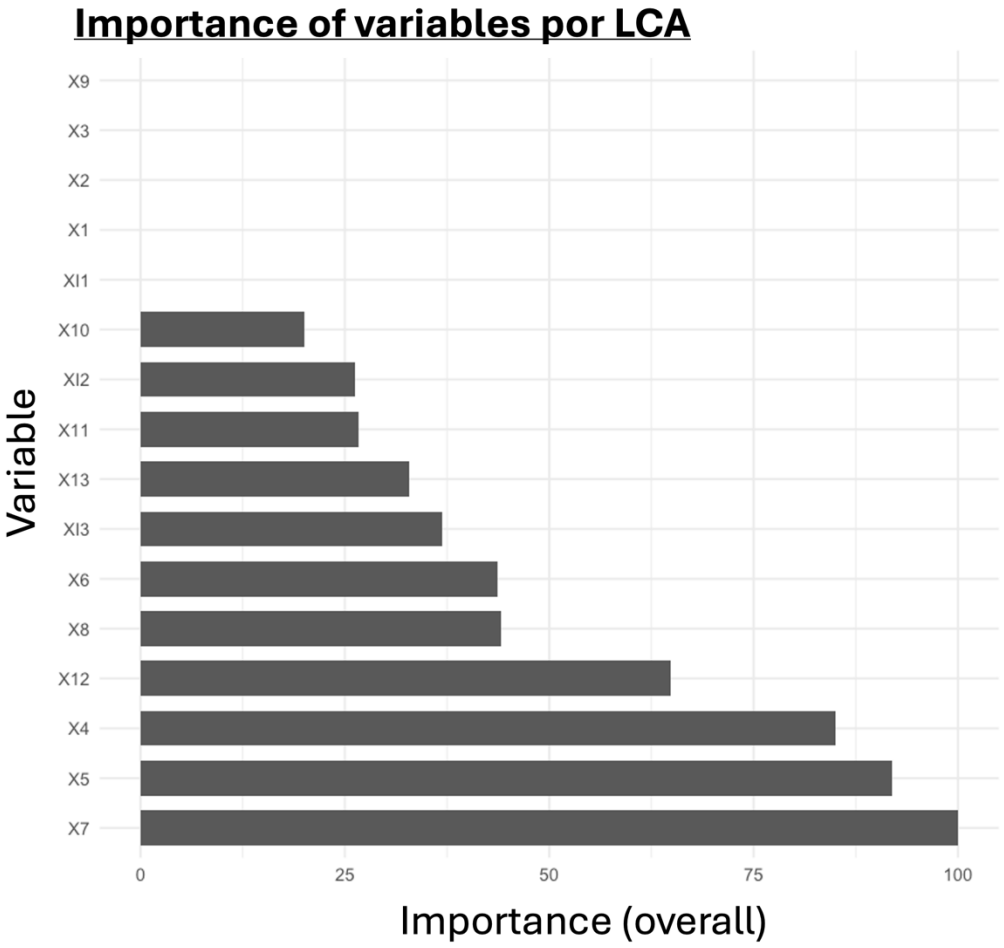

Figure S4. Relative importance of variables included in the predictive model for the proximity between ablation lesions and the right coronary artery (RCA) ostium, based on segmentation obtained by computed tomography. Variable codes are defined in Table S1.

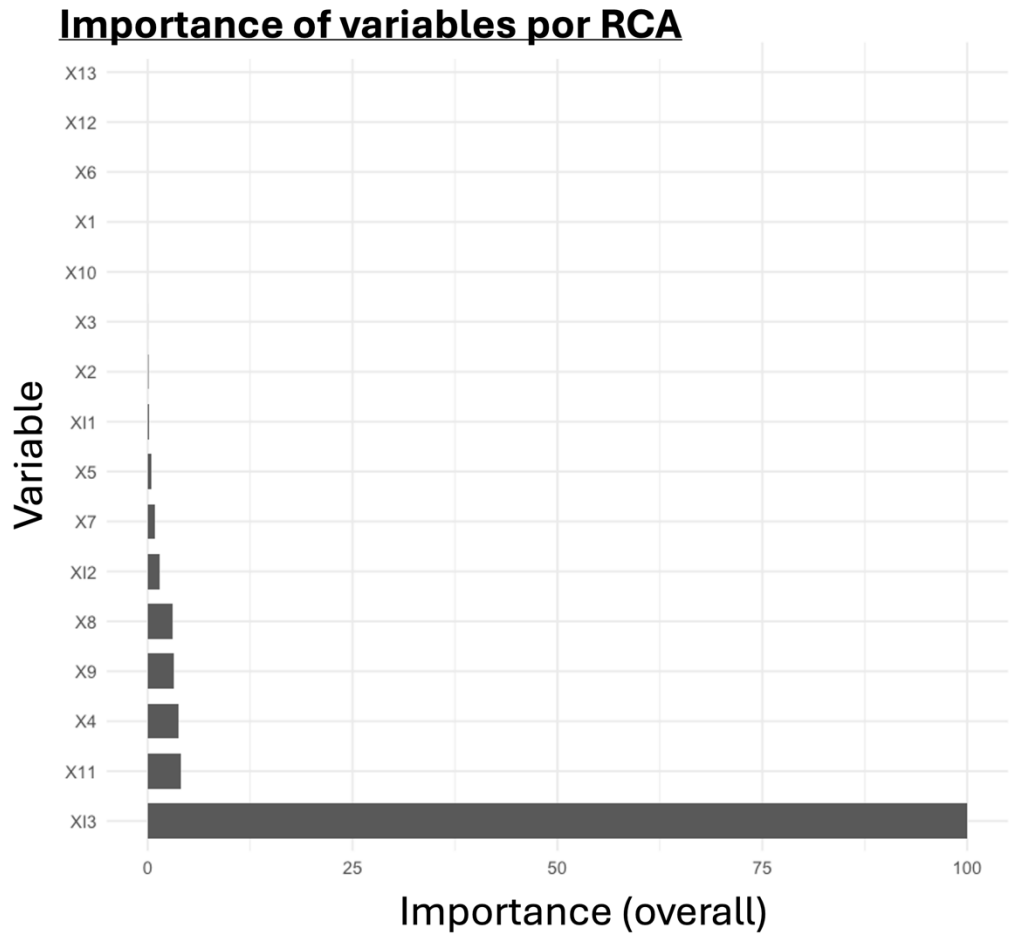

Figure S5. Model performance for estimating the distance to the right coronary artery (RCA).

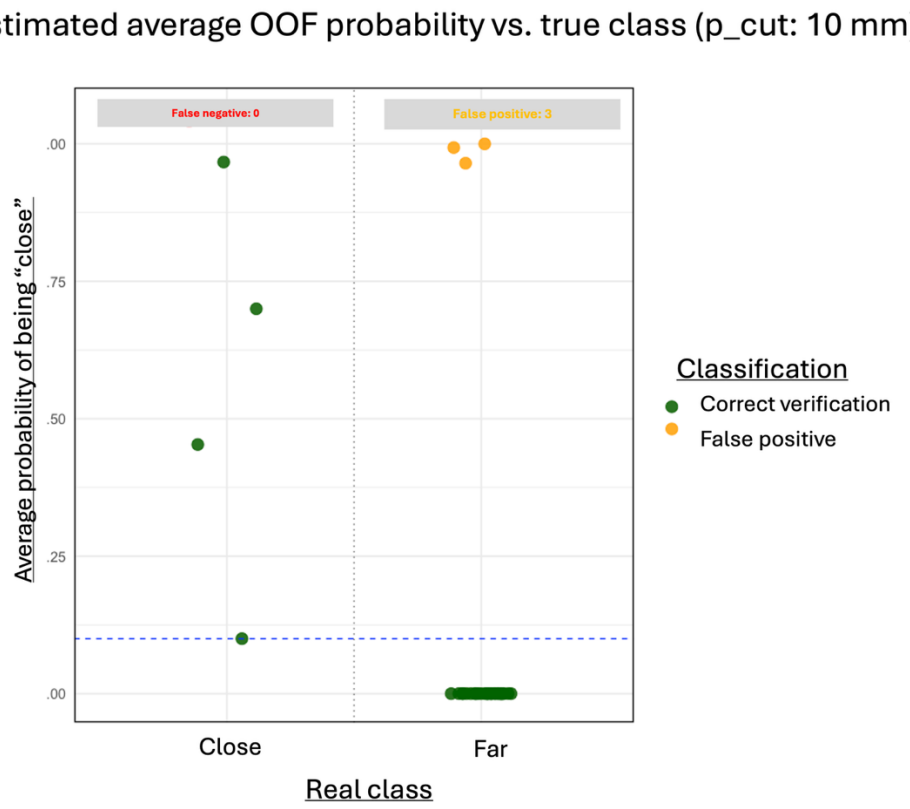

Figure S6. Model performance for estimating the distance to the left coronary artery (LCA).

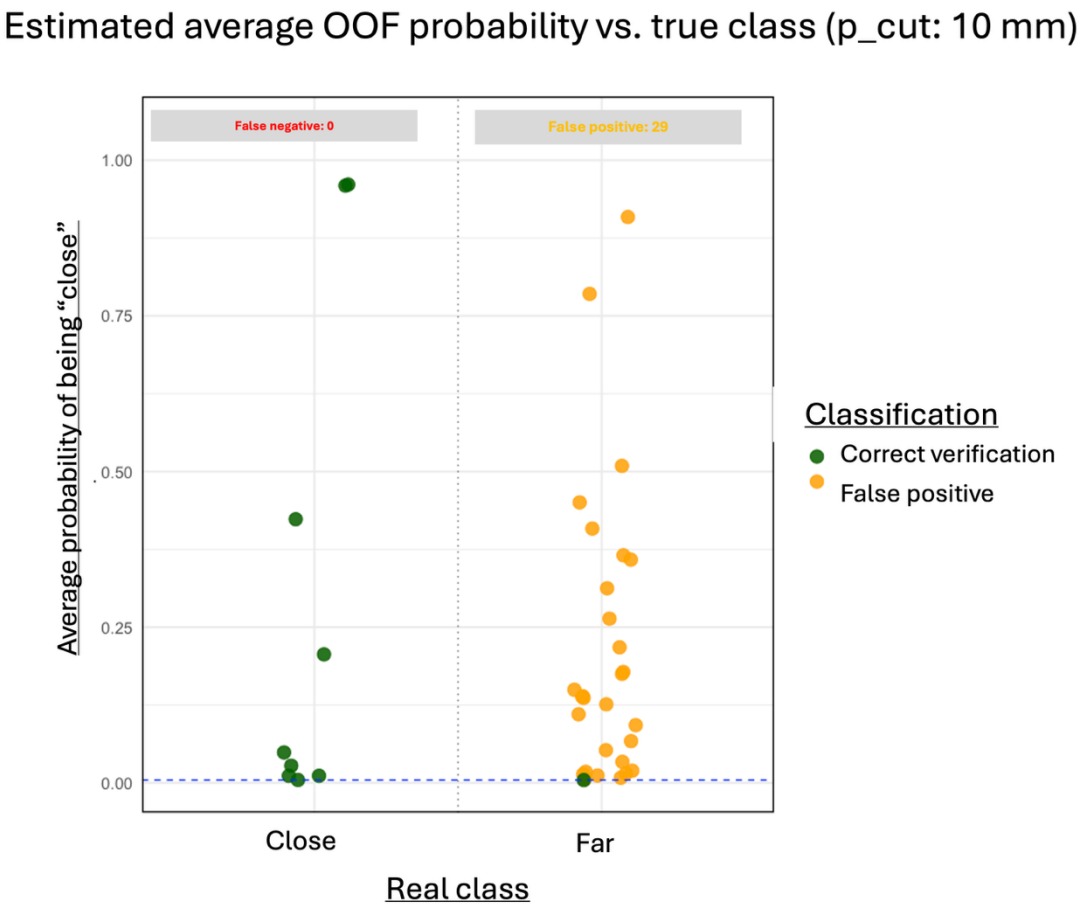

Figure S7: Mapped arrhythmia site of origin. Activation mapping was performed in all patients to identify the SOO of premature ventricular contractions, targeting the earliest local bipolar electrogram. Unipolar QS morphology and pace mapping were also assessed but considered adjunctive to bipolar activation timing. The diagram of the cardiac base shows the distribution of SOOs in the 51 included cases: 24 at the anterior intercommissural region (green circles), 10 at the left coronary cusp (yellow circle), 7 at the ventricular summit (pink circles), 7 at the right coronary cusp (red circle), and 3 at the mitral-aortic continuity (blue circle). SOO = site of origin; Ao = aortic valve; Pv = pulmonic valve; Mv = mitral valve.